



Journal of Advanced Research in Fluid Mechanics and Thermal Sciences

Journal homepage:
https://semarakilmu.com.my/journals/index.php/fluid_mechanics_thermal_sciences/index
ISSN: 2289-7879



Heat Transfer Enhancement of Biomass Based Stirling Engine

Nik Kechik Mujahidah Nik Abdul Rahman¹, Syamimi Saadon^{1,*}, Mohd Hasrizam Che Man²

¹ Department of Aerospace Engineering, Faculty of Engineering, Universiti Putra Malaysia, 43400 Serdang, Selangor, Malaysia

² Mechanical Precision Engineering, Malaysia-Japan International Institute of Technology (MIIT), Universiti Teknologi Malaysia, Jalan Semarak, 54100 Kuala Lumpur, Malaysia

ARTICLE INFO

Article history:

Received 15 April 2022

Received in revised form 20 August 2022

Accepted 1 September 2022

Available online 26 September 2022

Keywords:

Biomass; waste heat recovery; low temperature; biomass; Stirling engine

ABSTRACT

Stirling engine as an external combustion engine with high efficiencies and able to use any types of heat source is the best candidate to recover waste heat of the exhausted gas by converting it into power. Thus, in this study Stirling engine was introduced to evaluate the possibility of recovering waste heat from biomass to produce power. For this reason, Computational Fluid Dynamic (CFD) simulation test was performed to design an initial computational model of Stirling engine for low temperature heat waste recovery. The CFD model was validated with the experiment model and shows 6.11% of average deviation. This result proves that the computational model can be further used to evaluate the performance of Stirling engine as waste heat recovery of biomass-based industrial boilers for low-grade temperature heat source.

1. Introduction

Since Malaysia is one of the largest palm oil producers in the world, biomass has an advantage over other types of renewable energy replacing coal or natural gas in order to reduce carbon dioxide emissions [1]. For developing country like Malaysia, switching to renewable energy sources like biomass is critical to ensure the energy security of energy supply [2]. In the process of using biomass as energy source, biomass pellets are used for domestic water heating, co-firing of pulverized biomass and coal for electricity generation. For most industrial boilers using biomass, the range of thermal efficiency is 60-90%. For most industrial boilers using biomass, the range of thermal efficiency is 60-90%. Industrial boilers have a large fraction of thermal energy lost to the atmosphere while using biomass to produce electricity. The temperature of the exhaust flue gas range is low between 150-180°C (423.15 - 453.15K) [3], and in some cases it can reach up to 220°C (493.15K). For that reason, it has a significant potential to recover heat from the exhausted flue gas. It is important to recover heat as much as possible for environmental protection and energy conservation [4].

Compared to steamed engines, Stirling engine as an external combustion engine is known for its ability to use any kind of heat source including solar, biological, geothermal, or even industrial waste

* Corresponding author.

E-mail address: mimisaadon@upm.edu.my

heat [5]. Because of its high efficiencies and quite operation, Stirling engine has a great ability to recover low temperature waste heat from flue gas and convert it into power [6]. Nevertheless, the performance of the Stirling engine will decrease if attached with low temperature heat sources; between 200-500°C according to Bianchi and Pascale [7]. Therefore, study to enhance the heat transfer in the Stirling engine with low temperature biomass heat sources should be taken into consideration.

The energy to power the Stirling engine movement is completely driven by an external source of energy, generating work from the expansion and the compression of the working fluid, whereas energy in form of heat is added externally to the expansion chamber and removed from the compression chamber due to a differential temperature [8]. Thus, the losses of heat happening during the heat transfer process in and out of the engine become important [9]. Stirling engine as an external combustion engine, which means the energy used to power the engine movement is entirely obtained from the external source, the losses due to the heat transfer in and out of engine or due to the heat bypass within the engine structure may be more important than that the mechanical losses [9]. The method to increase heat transfer performance is known as heat transfer enhancement [10]. Hence, in order to achieve maximum efficiency of heat transfer for the best performance of the engine, it is crucial to study methods for heat transfer enhancement for the external part of the tubular heater [11]. Earlier works have been done to study and explore the behaviour of this external heat transfer by adding different materials as heat transfer enhancement [12]. However, a more accurate validation is needed to strengthen the numerical result.

Hence, this study is linking the gap of lacking research in studying the external part of tubular heater. Few researches have been done related to external part of the tubular heater of Stirling engine, disregarding the importance of this part in enhancing heat transfer as an external combustion engine. Apart from the experimental method that is widely used in modelling the optimum heat enhancement techniques in Stirling engine, numerical modelling also is widely used before performing the experimental model method [13]. Stirling engine consists of many multi-dimensional components which have significant geometrical effects to resolve the numerical models accurately. Computational Fluid Dynamic (CFD) approach is one of the numerical models that can simulate the multi-dimensional components and complicate processes in Stirling engine, hence gives an accurate prediction on the overall engine performance [5]. Therefore, CFD analysis is used to perform this study.

In this study, Stirling engine is introduced to evaluate the possibility of recovering waste heat from biomass to produce power. This paper presents the initial model of Stirling engine for further improvisation for low temperature heat transfer process from the biomass heat source to the external part of the tubular heater of the Stirling engine. This paper shows the validation of the baseline model of Stirling engine according to the previous researcher by applying different engine speed and comparing the trend lines of the power output based on every engine speed. This work is useful for further research in heat transfer enhancement of Stirling engine for low temperature heat source.

2. Methodology

2.1 Governing Equations

The flow field and heat transfer phenomena that happen in Stirling engine can be described mathematically by transient axisymmetric compressible Navier-Stokes equations, conservation of energy equation, conservation of mass and ideal gas equations written as Eq. (1) to Eq. (8)

Mass equation

$$\frac{\partial \rho_f}{\partial t} + \frac{\partial}{\partial x}(\rho_f \tilde{u}) + \frac{1}{r} \frac{\partial}{\partial r}(\rho_f r \tilde{v}) = 0 \quad (1)$$

The momentum

$$\begin{aligned} \frac{\partial}{\partial t}(\rho_f u) + \frac{\partial}{\partial x}(\rho_f \tilde{u}u) + \frac{1}{r} \frac{\partial}{\partial r}(\rho_f r \tilde{v}u) &= \rho_f g - \frac{\partial p}{\partial x} + \mu \frac{\partial}{\partial x} \left(\frac{\partial u}{\partial x} \right) + \frac{u}{r} \frac{\partial}{\partial r} \left(r \frac{\partial u}{\partial r} \right) + \frac{\mu}{3} \frac{\partial}{\partial x} (\nabla \cdot V) \\ \frac{\partial}{\partial t}(\rho_f v) + \frac{\partial}{\partial x}(\rho_f \tilde{u}v) + \frac{1}{r} \frac{\partial}{\partial r}(\rho_f r \tilde{v}v) &= -\frac{\partial p}{\partial r} + \mu \frac{\partial}{\partial x} \left(\frac{\partial v}{\partial x} \right) + \frac{u}{r} \frac{\partial}{\partial r} \left(r \frac{\partial v}{\partial r} \right) + \frac{\mu}{3} \frac{\partial}{\partial r} (\nabla \cdot V) - \frac{\mu v}{r^2} \end{aligned} \quad (2)$$

Energy conservation

$$\begin{aligned} \frac{\partial}{\partial t}(\rho_f T_f) + \frac{\partial}{\partial x}(\rho_f \tilde{u}T_f) + \frac{1}{r} \frac{\partial}{\partial r}(\rho_f r \tilde{v}T_f) &= -\frac{1}{c_{pf}} \left[\frac{\partial p}{\partial t} + \nabla \cdot (pV) - p(\nabla \cdot V) \right] + \frac{k_f}{c_{pf}} \left[\frac{\partial}{\partial x} \left(\frac{\partial T_f}{\partial x} \right) + \right. \\ &\left. \frac{1}{r} \frac{\partial}{\partial r} \left(r \frac{\partial T_f}{\partial r} \right) \right] + \frac{\mu}{c_{pf}} \left\{ 2 \left[\left(\frac{\partial u}{\partial x} \right)^2 + \left(\frac{\partial v}{\partial r} \right)^2 + \left(\frac{v}{r} \right)^2 \right] + \left(\frac{\partial v}{\partial x} + \frac{\partial u}{\partial r} \right)^2 - \frac{2}{3} (\nabla \cdot V)^2 \right\} \end{aligned} \quad (3)$$

Ideal gas equation

$$\rho V = \rho_f R T_f \quad (4)$$

Displacement of piston and displacer

$$X_p(t) = L_{pt} + R_d \sin \theta + \left[l_2^2 - \left(\frac{L}{2} - \frac{l_1}{2} - R_d \cos \theta \right)^2 \right]^{0.5} \quad (5)$$

Velocity of piston and displacer

$$X_d(t) = L_{dt} + R_d \sin \theta + \left[l_2^2 - \left(\frac{L}{2} - \frac{l_1}{2} - R_d \cos \theta \right)^2 \right]^{0.5} \quad (6)$$

Velocity of the piston

$$u_p(t) = R_d \omega \left\{ \cos \theta - \sin \theta \left[l_2^2 - \left(\frac{L}{2} - \frac{l_1}{2} - R_d \cos \theta \right)^2 \right]^{-0.5} \left[\frac{L}{2} - \frac{l_1}{2} - R_d \cos \theta \right] \right\} \quad (7)$$

Velocity of the displacer

$$u_d(t) = R_d \omega \left\{ \cos \theta + \sin \theta \left[l_2^2 - \left(\frac{L}{2} - \frac{l_4}{2} - R_d \cos \theta \right)^2 \right]^{-0.5} \left[\frac{L}{2} - \frac{l_4}{2} - R_d \cos \theta \right] \right\} \quad (8)$$

2.2 Modelling and Geometry

Computational fluid dynamics (CFD); ANSYS Fluent 20.1 software is used in this study to solve the continuity, momentum and energy. To include the conduction heat transfer through external wall, the wall features and thickness were detailed in the wall boundary condition. There are very few computational works in the literature that fully provides complete information about geometry and boundary conditions that is needed to design geometry for the CFD simulations. The computational

analysis from Ben-Mansour *et al.*, [14] is referred for the initial geometry of Stirling engine model since it provides a concise information needed for the CFD simulation.

A rhombic drive mechanism of β -type Stirling engine which consists of three zones; compression zone, expansion zone, and narrow zone as shown in Figure 1 is arrogated as a reference. The narrow zone that connects the expansion and compression zone is assumed to have no regenerator materials. The dimensions of the geometries are listed in Table 1.

Table 1
 Dimension of simulated geometry of the Stirling engine in (mm) [14]

Working fluid	Air
r_1	43
r_2	42.25
l_d	155
$l_1 = l_2 = l_3 = l_4$	66
R_d (mm)	$l_1/2.6666$
L_{pt}	50.93
L_{dt}	163.74
R_d	3.5
Engine speed	360-500rpm

The simulation model of Stirling engine is solved as 3D geometry as shown in Figure 2. Air is utilized and treated as an ideal gas in this study. Air is assumed to be dependent on the gas temperature. The dimension of simulated geometry of the Stirling engine is stated in Table 1. The cylinder wall features, and thickness is detailed in the wall boundary condition is as shown in Table 2. The thermal boundary conditions are between 775K for hot temperature (T_H) and 300K for cold temperature (T_C).

Table 2
 Cylinder wall dimensions and properties [14]

Thickness (mm)	1
Material	Steel
Density (kg/m^3)	7840
Thermal conductivity ($\text{Wm}^{-1} \cdot \text{k}^{-1}$)	43
Specific heat ($\text{J} \cdot \text{kg}^{-1} \cdot \text{K}^{-1}$)	450

The engine will start to move when there is a source of heat at the cylinder head. The displacer is a loose fit; its job is to shuttle air back and forth within the cylinder. The air within the cylinder is forced upward to the hot end of the engine while the displacer travels towards the cold end. The air heats up, expands, and the power piston is pushed towards the crankshaft as a result. The air is forced to the cold side of the cylinder as the displacer travels towards the hot end. The power piston is pulled inwards, away from the crankshaft, as the air cools and contracts [15].

Further analysis on the work done by the engine is performed and compared with the experimental data of work done reported by Aksoy and Cinar [16] to ensure that the model is viable. The model then will be used for further evaluation with lower temperature of heat sources.

Geometry of Stirling engine used in CFD simulation is generated in Solidworks 2019. Figure 2(b) shows physical domain of Stirling engine with outer diameter of 90 mm and height of 213.12 mm. The displacer is located 13.98 mm from the bottom surface, has diameter of 132.73 mm and height of 155 mm.

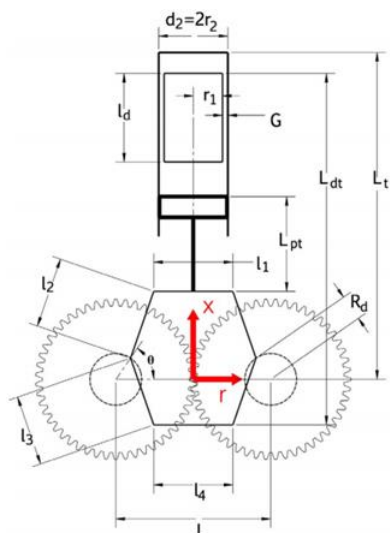


Fig. 1. Engine configuration [14]

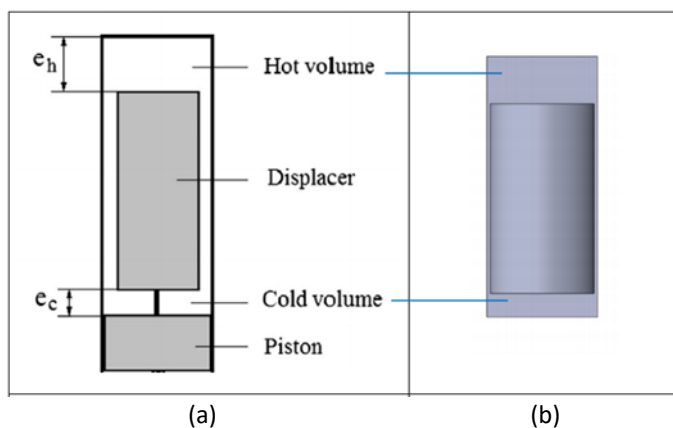
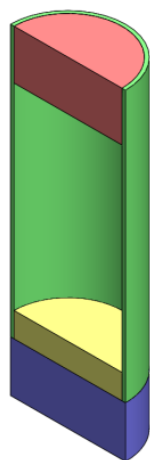


Fig. 2. (a) Schematic diagram and (b) CFD Domain

2.2 Mesh and Boundary Condition Setup

To have a better control of mesh generated and to reduce computational Stirling engine domain is divided into four sub-domains (volumes) to simplify the analysis. The volumes were named as displacer top volume, displacer bottom volume, engine gap volume and piston volume as shown in Figure 3.



	1. Displacer top volume
	2. Displacer bottom volume
	3. Engine gap volume
	4. Piston Volume

Fig. 3. Four volumes of Stirling engine generated in crosscut at mid-plane

The layering dynamic mesh function and user-defined function (UDF) is applied for the movement of the piston and displacer at transient condition. Air is utilized as working fluid and set as the ideal gas. For the validation model, the thermal boundary condition for the heating surface is 775K and 300K for the piston surface. The basis pressure is in the Stirling engine cycle for this study is 1 atm. The analysis is pressure based with unsteady RANS (URANS). Analysis performed with k-omega SST turbulence model with Energy model is turned on. The equations then were discretized with the Coupled Scheme Pressure-velocity coupling algorithm because it shows a relatively fast convergence compared to SIMPLE scheme [17]. For the density, momentum and energy equations, the second-order upwind scheme is used while the first-order upwind scheme is used for the turbulent kinetic energy and specific dissipation rate.

Figure 4(a) shows overall mesh in this study, with minimum and maximum cells size are 1.5mm and 4 mm, respectively. Minimum cells size is for the regenerator area (gap) between displacer and engine that is so narrow and very crucial to apply dense mesh. All the mesh generated using structured mesh with combination of hexahedral and quadrilateral 3D elements with total cell number of 87,882. Figure 4(b) shows mesh at the gap between displacer and engine gap with element size of 1.5 mm. Temperature source defined in boundary condition as shown in Figure 5 for (a) hot surface and (b) cold surface.

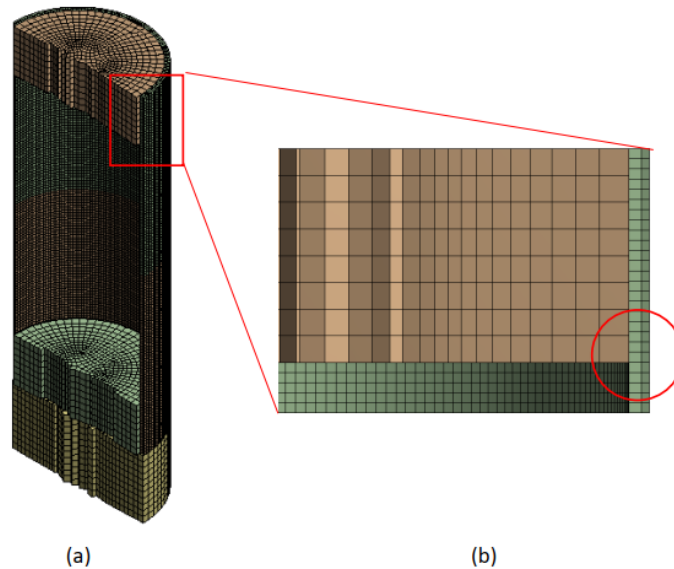


Fig. 4. Mesh generated for this study (a) overall mesh (b) refined mesh at the engine gap

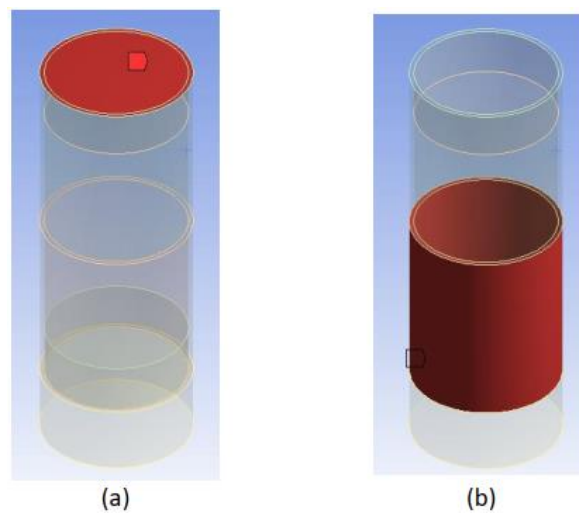


Fig. 5. Two boundary conditions for heat source (a) hot surface and (b) cold source surface

3. Results

3.1 Validation of the Stirling Engine Model

This section discusses the results of Stirling engine validation. The model was previously validated in our previous study [18]. However, in this paper, in order to ensure the validity of the power calculation versus the engine speed, the model is once again verified by comparing the simulation

results obtained from this study with the experimental results that were obtained in the study by Aksoy and Cinar [16]. Figure 6 shows the comparison of engine power-engine speed relation of experimental result and CFD result obtained from this study. The engine power is calculated by multiplying the engine work done with rotational engine speed per minute. The work done by the system can be derived by integrating the area of this P-V diagram. The pressure value is taken from the pressure in the cold volume every time step of the engine cycle. While the volume is the area of the displacer surface and the height of cold volume in every time step. From this result, the trend lines are sketched in Figure 6. From the trend lines of CFD data and experimental data in Figure 6, engine speed of 440-525 rpm, cold source temperature of 300K, and hot source temperature of 775K were determined.

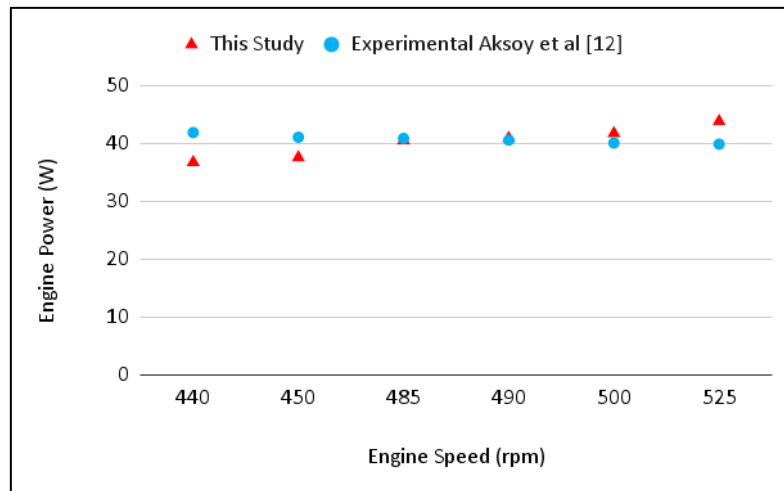


Fig. 6. Engine speed vs power

For CFD results, maximum engine power was found to be 43.75W at 525 rpm of engine speed. While the minimum engine power obtained was 36.67W at 440 rpm engine speed. From Table 3, we can observe that the smallest deviation of 0.82% is found when the engine speed is at 490 rpm. While the largest deviation of 12.28% when the engine speed is at 440 rpm. The overall comparison of the trend lines of experimental result and CFD result shows average deviation of 6.11% for every engine speed applied. Although the comparison result shows a small deviation, as the preliminary result, it can be further improved and exploited to determine the best method for the heat transfer in Stirling engine especially from the heat source into the top volume of the Stirling engine.

Table 3

Cylinder wall dimensions and properties

Engine Speed (rpm)	CFD-Engine Power (W)	Experimental-Engine Power (W)	Deviation%
440	36.67	41.8	12.28
450	37.5	41	8.54
485	40.42	40.8	0.94
490	40.83	40.5	0.82
500	41.67	40.0	4.17
525	43.75	39.8	9.92

The final total temperature distribution profile for every engine speed applied is shown in Figure 7(a) to Figure 7(f) below. From the CFD simulation plotted, the results obtained shows that the difference of the power output with experimental value is small for engine speed 485 rpm, 490 rpm and 500 rpm. As shown in Figure 8, turbulence swirl of higher temperature heat starts to form within the hot volume when engine speed is 485 rpm. This indicates that for higher engine speed, the fluid

is in a good state of thermal performance in expansion zone. Meanwhile, the results obtained for engine speed 440 rpm and 450 rpm shown in Figure 7(a) and Figure 7(b) give an understandable point that heat is unevenly distributed between the expansion and compression zone in the cylinder wall. This is also a not very outstanding thermal performance of fluid throughout the cylinder. As shown in Figure 7(c), Figure 7(d) and Figure 7(e) quite good temperature and heat distributions are achieved for engine speed 485 rpm, 490 rpm and 500 rpm.

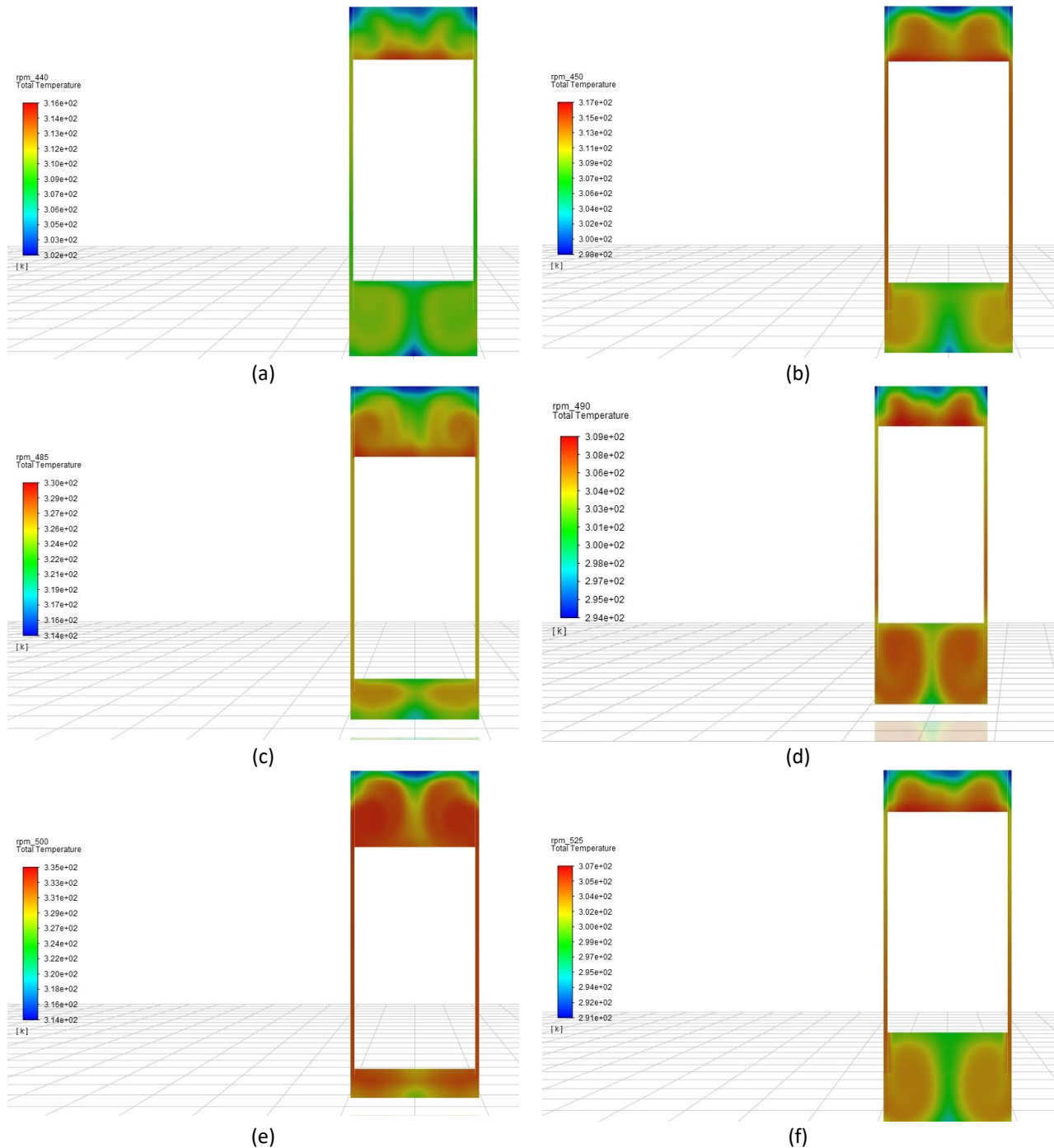


Fig. 7. Total temperature distribution (a) 440rpm (b) 450rpm (c) 485rpm (d) 490rpm (e) 500rpm (f) 525rpm

It can be observed that the surface area is important for the heat to establish an actual fluid flow towards the expansion zone which is located at the upper part of the cylinder. It can be seen clearly that results achieved when engine speed is 485, 490 and 500 rpm are the most suitable for the CFD

model to get the nearest power output value to the experimental result. From all the results above, one can observe that significant criteria of parameter in this study would be the suitable engine speed in CFD model to get the minimum deviation percentage from the actual experimental value.

4. Conclusions

The validation of the baseline model of Stirling engine according to the previous researchers is presented in this study. The validation is conducted by applying different engine speed and comparing the trend lines of the power output based on every engine speed. It shows that the CFD results obtained in this study is deviated 6.11% from the actual experimental results. The details of the temperature distribution within the engine's wall are also described in here so that one can understand better the effect of the different engine speed to the engine's power output.

From the validated model obtained, further study could be done on the Stirling engine model by studying different parameters analysis especially focusing on the engine wall area. This part can be modified by using different types of material; in order to enhance the heat transfer process and eventually the power output of the engine.

Acknowledgement

This research was funded by a grant from Ministry of Higher Education of Malaysia (FRGS Grant: FRGS/1/2018/TK07/UPM/02/2).

References

- [1] Abdullah, Wan Syakirah Wan, Miszaina Osman, Mohd Zainal Abidin Ab Kadir, and Renuga Verayiah. "The potential and status of renewable energy development in Malaysia." *Energies* 12, no. 12 (2019): 2437. <https://doi.org/10.3390/en12122437>
- [2] Ilham, Zul, Nur Aida Izzaty Saad, Wan Abd Al Qadr Imad Wan-Mohtar, and Adi Ainurzaman Jamaludin. "Multi-criteria decision analysis for evaluation of potential renewable energy resources in Malaysia." *Progress in Energy and Environment* 21 (2022): 8-18. <https://doi.org/10.37934/progee.21.1.818>
- [3] Dehghan, Babak, Linwei Wang, Mario Motta, and Nader Karimi. "Modelling of waste heat recovery of a biomass combustion plant through ground source heat pumps-development of an efficient numerical framework." *Applied Thermal Engineering* 166 (2020): 114625. <https://doi.org/10.1016/j.applthermaleng.2019.114625>
- [4] Li, Feng, Lin Duanmu, Lin Fu, and Xi ling Zhao. "Research and application of flue gas waste heat recovery in co-generation based on absorption heat-exchange." *Procedia Engineering* 146 (2016): 594-603. <https://doi.org/10.1016/j.proeng.2016.06.407>
- [5] Chen, Wen-Lih, King-Leung Wong, and Yu-Feng Chang. "A computational fluid dynamics study on the heat transfer characteristics of the working cycle of a low-temperature-differential γ -type Stirling engine." *International Journal of Heat and Mass Transfer* 75 (2014): 145-155. <https://doi.org/10.1016/j.ijheatmasstransfer.2014.03.055>
- [6] Song, Zhengchang, Jianmei Chen, and Li Yang. "Heat transfer enhancement in tubular heater of Stirling engine for waste heat recovery from flue gas using steel wool." *Applied Thermal Engineering* 87 (2015): 499-504. <https://doi.org/10.1016/j.applthermaleng.2015.05.028>
- [7] Bianchi, Michele, and Andrea De Pascale. "Bottoming cycles for electric energy generation: Parametric investigation of available and innovative solutions for the exploitation of low and medium temperature heat sources." *Applied Energy* 88, no. 5 (2011): 1500-1509. <https://doi.org/10.1016/j.apenergy.2010.11.013>
- [8] Schneider, T., D. Müller, and J. Karl. "A review of thermochemical biomass conversion combined with Stirling engines for the small-scale cogeneration of heat and power." *Renewable and Sustainable Energy Reviews* 134 (2020): 110288. <https://doi.org/10.1016/j.rser.2020.110288>
- [9] Hsieh, Y. C., T. C. Hsu, and Jenq-Shing Chiou. "Integration of a free-piston Stirling engine and a moving grate incinerator." *Renewable Energy* 33, no. 1 (2008): 48-54. <https://doi.org/10.1016/j.renene.2007.01.015>
- [10] Siddique, M., A-RA Khaled, N. I. Abdulhafiz, and A. Y. Boukhary. "Recent advances in heat transfer enhancements: a review report." *International Journal of Chemical Engineering* 2010 (2010). <https://doi.org/10.1155/2010/106461>
- [11] Saadon, S. "Possibility of Using Stirling Engine as Waste Heat Recovery-Preliminary Concept." In *IOP Conference Series: Earth and Environmental Science*, vol. 268, no. 1, p. 012095. IOP Publishing, 2019.

- <https://doi.org/10.1088/1755-1315/268/1/012095>
- [12] Helman, Harlinda, and Syamimi Saadon. "Design and Modelling of a Beta-Type Stirling Engine for Waste Heat Recovery." *Journal of Advanced Research in Fluid Mechanics and Thermal Sciences* 64, no. 1 (2019): 135-142.
- [13] Cheng, Chin-Hsiang, and Yen-Fei Chen. "Numerical simulation of thermal and flow fields inside a 1-kW beta-type Stirling engine." *Applied Thermal Engineering* 121 (2017): 554-561. <https://doi.org/10.1016/j.applthermaleng.2017.04.105>
- [14] Ben-Mansour, R., A. Abuelyamen, and Esmail M. A. Mokheimer. "CFD analysis of radiation impact on Stirling engine performance." *Energy Conversion and Management* 152 (2017): 354-365. <https://doi.org/10.1016/j.enconman.2017.09.056>
- [15] Kumaravelu, Thavamalar, and Syamimi Saadon. "Heat transfer enhancement of a Stirling engine by using fins attachment in an energy recovery system." *Energy* 239 (2022): 121881. <https://doi.org/10.1016/j.energy.2021.121881>
- [16] Aksoy, Fatih, and Can Cinar. "Thermodynamic analysis of a beta-type Stirling engine with rhombic drive mechanism." *Energy Conversion and Management* 75 (2013): 319-324. <https://doi.org/10.1016/j.enconman.2013.06.043>
- [17] Abuelyamen, A., R. Ben-Mansour, H. Abualhamayel, and Esmail MA Mokheimer. "Parametric study on beta-type Stirling engine." *Energy Conversion and Management* 145 (2017): 53-63. <https://doi.org/10.1016/j.enconman.2017.04.098>
- [18] Rahman, Nik Kechik Mujahidah Nik Abdul, Syamimi Saadon, and Mohd Hasrizam Che Man. "Waste Heat Recovery of Biomass Based Industrial Boilers by Using Stirling Engine." *Journal of Advanced Research in Fluid Mechanics and Thermal Sciences* 89, no. 1 (2022): 1-12. <https://doi.org/10.37934/arfmts.89.1.112>